Global Approach to the Spectral Problem of Microinstabilities in Tokamak Plasmas using a Gyrokinetic Model

S.Brunner, M.Fivaz and J.Vaclavik

Centre de Recherches en Physique des Plasmas

Association Euratom - Confédération Suisse

Ecole Polytechnique Fédérale de Lausanne/ PPB - CH-1015 Ecublens/Switzerland

Abstract

A gyrokinetic eigenvalue code has been developed for computing global ion temperature gradient (ITG) -related instabilities in tokamak configurations. Although trapped ion dynamics are not yet considered in this model, it contains full finite Larmor radius and finite orbit width effects of circulating ions. Non-adiabatic trapped electron dynamics are included through a bounce-averaged drift kinetic equation. Differences between the local ballooning approximation and the global approach are presented and discussed. The possible coupling between the trapped electron mode (TEM) and the toroidal-ITG mode is also investigated. Finally, the evolution of the spectrum of these different instabilities is studied for varying central negative magnetic shear configurations.

Introduction: For studying microinstabilities in tokamak-like plasmas, most linear kinetic studies were carried out for high toroidal wave numbers using the ballooning representation[1] which leads to a one-dimensional integral equation along the magnetic field lines. Except for very few cases, these calculations do not include a higher order WKB procedure for determining the radial structure. Thus these results usually stay local to a magnetic surface and there remains some questioning on the actual radial extent of these modes. For low toroidal wave numbers where the ballooning representation breaks down and the full two-dimensional problem cannot be reduced, very little linear computation has been carried out. This limit is of interest as it describes larger wavelength fluctuations which could lead to higher turbulent transport. Until recently the only published results from true global, linear computations came from a spectral code by Marchand, Tang and Rewoldt[2]. This model contains no finite Larmor radius (FLR) effects and is based on a second order expansion with respect to the radial excursion of trapped particles, which leads to spurious modes[3] and thus to a difficult search of physical eigenfrequencies. At the present state full non-linear simulations already exist[4][5], nonetheless there remains a need for global linear studies as they enable to determine more accurately the conditions of marginal stability and in this way, if possible, to find stable configurations. This has prompted us to undertake the development of a new, global, spectral gyrokinetic code. A summary of the present state physical model as well as of first results is given here. More details are found in Ref.[6].

Physical Model for the Spectral Approach

Geometry: At present the geometry of the system is still approximated by a large aspect ratio torus with circular, concentric magnetic surfaces. Therefore finite pressure effects such as the Shafranov shift are not taken into account. The safety factor profile $q_s(\rho)$, the ion and electron temperature profiles $T_{e,i}(\rho)$ as well as the density profile $N(\rho)$ are chosen arbitrarily and in this way are represented by simple polynomial functions of the radial variable ρ. Here (ρ, θ, φ) is the standard set of toroidal coordinates.

Kinetic equations: Although the basic mechanism of ITG instabilities can be described by fluid models, the more detailed behavior of these perturbations also contain specifically kinetic characters, such as wave-particle interaction (e.g. Landau damping) and FLR effects. In order to take them into account - this being essential if one is interested in determining accurately conditions of marginal stability- appropriate kinetic equations for each species must be considered. Assuming a collisionless plasma, these can be derived by reducing the Vlasov equation, linearized for electrostatic perturbations, using different scaling laws. In particular, as microinstabilities have low frequencies i.e. small compared to the cyclotron frequencies $\Omega_{e,i}$, one can for all particles carry out a gyroaveraging procedure.

In the case of **ions** the Larmor radius can be comparable or larger then the wavelengths perpendicular to the magnetic field, giving rise to the above mentioned FLR effects. The appropriate equation of motion is thus given by the gyrokinetic equation (GKE) [7]:

$$\left.\frac{D}{Dt}\right|_{u.t.GC} \tilde{g} = \left[\frac{\partial}{\partial t} + \vec{v}_{GC} \cdot \frac{\partial}{\partial \vec{R}}\right] \tilde{g} = -i\frac{q}{T} F_M(\omega - \omega^\star) < \phi >_g ,$$

where $D/Dt|_{u.t.GC}$ stands for the total time derivative along the unperturbed trajectories $\vec{R}(t)$ of the guiding centers (GC), including drifts related to the gradient and curvature of the magnetic field. Furthermore, $\tilde{g}$ represents the fluctuating, non-adiabatic part of the particle distribution function written in gyro-center variables, F_M the local Maxwellian distribution of equilibrium, $\omega^\star$ the diamagnetic frequency related to the temperature and density inhomogeneities and $< \phi >_g$ the gyroaveraged electrostatic potential.

In first approximation the mobile **electrons** have been assumed to respond adiabatically to the low frequency microinstabilities and therefore to follow a Boltzmann distribution. However in the non-trivial tokamak geometry, the trapped electrons in fact have a toroidal precessional drift which can become comparable to the phase velocity of the perturbation. To take into account the resonances which may arise, a more detailed

description has been considered. As electrons have significantly smaller Larmor radii then ions for similar temperatures, FLR effects can usually be neglected (at least when studying ion-driven instabilities), so that the drift kinetic equation (DKE) instead of the GKE is sufficient. Furthermore, due to the high thermal velocity of these particles, this equation can be averaged over the periodic motion in the poloidal plane, giving rise to the so-called bounce-averaged DKE[8]:

$$\left.\frac{D}{Dt}\right|_{u.t.B} \tilde{g}_b = \left[\frac{\partial}{\partial t} + <\dot{\varphi}>_b \frac{\partial}{\partial \varphi}\right] \tilde{g}_b = -i\frac{q}{T} F_M(\omega - \omega^*) < \phi >_b .$$

Here $D/Dt|_{u.t.B}$ stands for the total time derivative along the unperturbed trajectories of the banana (B) orbits, $\tilde{g}_b$ for the fluctuating, non-adiabatic part of the bounce-averaged GC distribution function, $<\dot{\varphi}>_b$ for the average toroidal precessional drift and $< \phi >_b$ for the bounce-averaged potential.

The equations of motion are solved by integrating along the unperturbed trajectories. In the case of ions the modulation of the magnetic field along the trajectory was neglected, so that in particular the dynamics of trapped ions was discarded. In its present state our model therefore still does not enable to describe trapped ion modes (TIM). In this context Fourier representation appears naturally as it enables to integrate explicitly the unknown potential ϕ. For example, when gyroaveraging the potential one obtains

$$< \phi >_g = < \int d\vec{k}\, \hat{\phi}\,(\vec{k},t)\, e^{i\vec{k}\cdot\vec{r}} >_g = \int d\vec{k}\, J_0\left(\frac{k_\perp v_\perp}{\Omega}\right) \hat{\phi}\,(\vec{k},t) e^{i\vec{k}\cdot\vec{R}},$$

where J_0 is the zero order Bessel function containing the full FLR effects and having used the relation $\vec{R} = \vec{r} + \vec{v} \times \vec{e}_{||}\,/\Omega$ between the GC and particle position. In fact, instead of a decomposition into plane waves, a Fourier representation in terms of toroidal wave components was chosen as it is more adapted to the geometry of the system:

$$\phi(\rho,\theta,\varphi;t) = \sum_{(\kappa,m)} \hat{\phi}_{(\kappa,m)} \exp i(\kappa\rho + m\theta + n\varphi - \omega t),$$

where κ is a radial, m a poloidal and n the fixed toroidal wave number. Note that a Fourier series decomposition instead of a Fourier transform is considered not only in the periodic direction θ but also along the radial coordinate ρ, this being justified by the finite dimension of the system. The fixed frequency is noted ω.

Eigenvalue equation: The equations of motion are completed with a relation for ϕ. This is provided by the quasineutrality equation (justified when studying low frequency microinstabilities), which leads to the actual eigenvalue equation for (ω, ϕ). It turns out

to be advantageous to solve this eigenvalue problem staying in the discrete Fourier space (κ, m). Indeed, the equation is then naturally discretized and contains no singularity as the one appearing in the kernel of the integral equation when solving in the continuous configuration space (ρ, θ). The eigenvalue problem can formally be written in matrix form:

$$\overleftrightarrow{M}(\omega)\,\vec{\phi} = 0.$$

This is not a standard problem as the matrix $\overleftrightarrow{M}$ has an intricate dependence in the eigenvalue ω. The characteristic equation for ω:

$$D(\omega) = \det \overleftrightarrow{M}(\omega) = 0, \qquad \omega \text{ complex},$$

is solved by taking advantage of the analyticity of $D(\omega)$ and using a practical method proposed by Davies[9]. By sampling $D(\omega)$ along a closed curve in the complex frequency plane, this approach allows not only to find the number of enclosed zeros using the principle of argument (Nyquist), but the value itself of these roots with great accuracy. In this way the full unstable spectrum of a given system can be computed quite effectively.

Results

Benchmarking with time evolution PIC code: The spectral code has been extensively benchmarked against another global, linear gyrokinetic code developed simultaneously at the CRPP, based on a time evolution particle in cell (PIC) method[10][11]. In the regime where trapped ion dynamics (contained in the PIC model) are not important, i.e. for frequencies above the average ion bounce frequency, and for not too short wavelengths (PIC model is only valid to second order in Larmor), comparisons have shown very good agreement. Details of this validation can be found in Ref.[12].

Comparison with local ballooning calculations: Results from the global spectral code have also been compared to those obtained by Dong et al.[13] applying the local ballooning approximation to the same physical model. In this case only the adiabatic response of trapped electrons is taken into account so that the instabilities are essentially toroidal-ITG. To carry out such a comparison, the profiles for the global code must be chosen such that they match the local ballooning parameters on a reference magnetic surface. Here these parameters are given by the safety factor q_s, the temperature ratio $\tau = T_e/T_i$, $\epsilon_n = L_n/R$ =characteristic length of density/ major radius, $\eta_i = L_n/L_{T_i}$ =charac.length of density/ charac.length of ion temperature and the normalized poloidal mode number

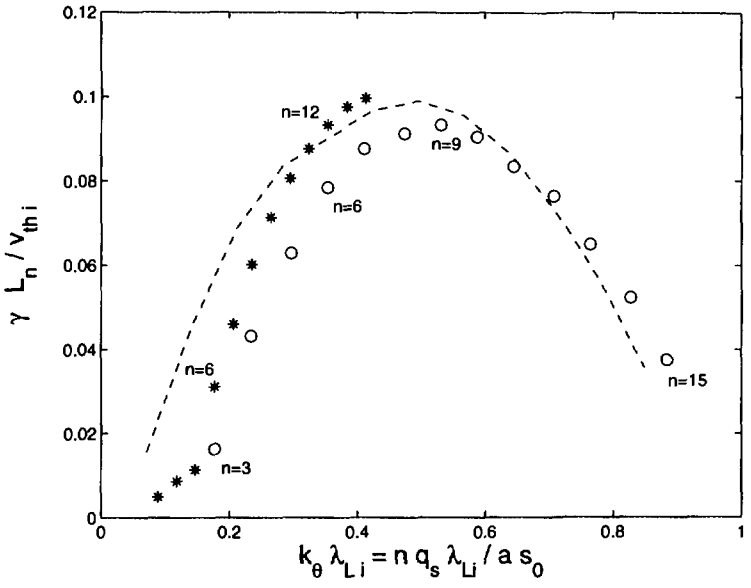

Figure 1: Growth rate γ as a function of $k_\theta \lambda_{Li}$ (only adiabatic response of electrons). Circles and stars represent global results for $a/\lambda_{Li} = 56.5$ and $a/\lambda_{Li} = 113.0$ respectively, a being the minor radius of the plasma. Labels below the circles and above the stars indicate the corresponding toroidal wave number. Ballooning results are reported here with a dashed line.

$\tilde{k_\theta} = nq_s\lambda_{Li}/\rho_0$, where λ_{Li} is the average ion Larmor radius on the reference magnetic surface $\rho = \rho_0$. Note that both, a high temperature plasma with a perturbation having low toroidal mode number n, or a low temperature and high n, can lead to a same value $\tilde{k_\theta}$ and thus be iso-dynamical with respect to the local ballooning calculation. Fig.1 presents the growth rates obtained when carrying out such a comparison along an n-scan. A hot as well as a cold plasma scenario have been considered when running the global code and in both cases the corresponding results indeed join the local ones for sufficiently high toroidal mode numbers, i.e. $n \gtrsim 10$. Ballooning results are from Fig.3 of Ref.[13]. The typical role over of the growth rate around $\tilde{k_\theta} \simeq 0.5$ is the consequence of FLR effects.

Effect of trapped electrons on the toroidal-ITG: The effect of non-adiabatic trapped electron dynamics is essentially twofold. In case of a flat density profile it simply strengthens the growth rate of the toroidal-ITG instability, which thus keeps its dominantly ion driven character. For non-flat density profiles (low values of ϵ_n and η_i) the toroidal-ITG can either couple and convert to, or simply be taken over by a trapped electron mode (TEM). This TEM may remain unstable down to flat ion temperature profiles, thus effectively removing the threshold on η_i predicted for the pure toroidal-ITG when only adiabatic electrons are considered. In this way our global results qualitatively

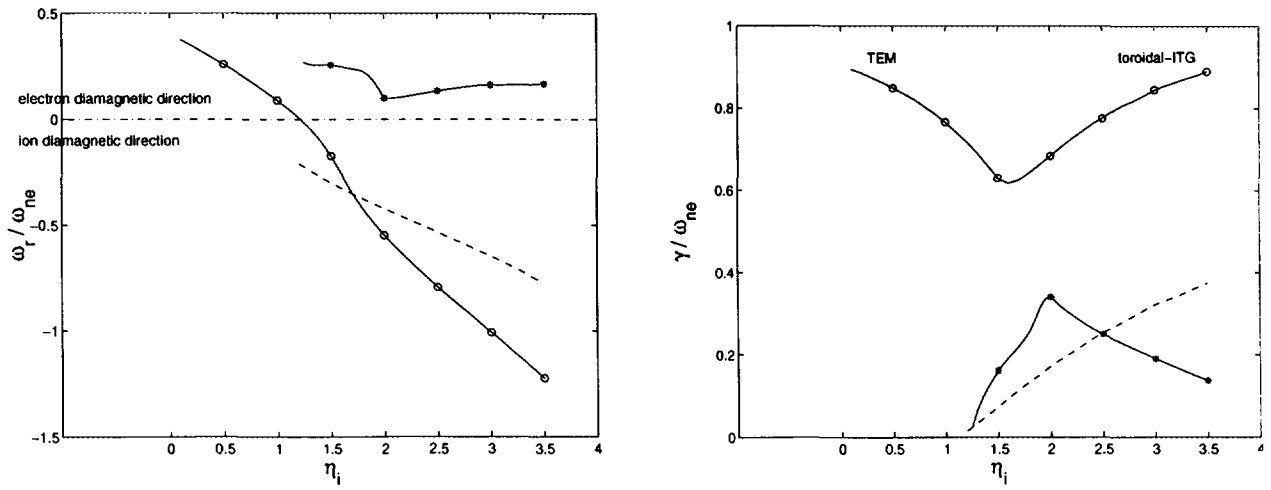

Figure 2: Real frequencies ω_r and growth rates γ of the most unstable eigenmodes as a function of η_i holding in particular $\epsilon_n = 0.2$=const and $\eta_e = 2$ =const, computed with non-adiabatic trapped electrons (full lines). For $\eta_i \lesssim 1$ the toroidal-ITG converts to a predominantly TEM (mode 1) and starts to propagate in the electron instead of the ion diamagnetic direction. A weaker instability propagating essentially in the electron diamagnetic direction (mode 2) is also present. For comparison, results with only adiabatic electrons are reproduced with dashed lines. Note how non-adiabatic trapped electron dynamics have removed the threshold on η_i.

confirm the picture given by Romanelli and Briguglio [14] solving a local dispersion relation. As an illustration, results of an η_i-scan are presented in Fig.2.

Negative shear scan: The global spectral code has been applied for studying the stabilizing effect of negative magnetic shear. Motivation for such studies come from experimental evidence on different tokamaks[15][16][17] of the formation of a transport barrier in regions of shear reversal accompanied by a reduction in core fluctuation amplitudes. Fig.3 presents the results of such a shear scan having fixed $n = 10$ and the profiles such that $\tau = 1$, $\epsilon_n = 0.25$, $\eta_i = \eta_e = 2.5$, $\tilde{k_\theta}$= 0.35, $\alpha_b = 45\%$ (fraction of trapped particles) on the magnetic surface $\rho = \rho_0$ where the modes tend to be centered (steepest gradients). The safety factor profile is varied such that $q_s(\rho_0) = 1.5$ is held fixed while shear varies from $\hat{s}\ (\rho_0) = +1$ to -1. For positive values of shear the spectrum contains eigenmodes propagating in the ion diamagnetic direction, i.e. having a dominantly toroidal-ITG character, as well as instabilities propagating in the electron diamagnetic direction, i.e. having essentially a TEM character. In this case, the TEM's are completely suppressed at negative shear $\hat{s}$= -1, while the toroidal-ITG modes are still present, their growth rate being nonetheless attenuated by a factor ~ 4 with respect

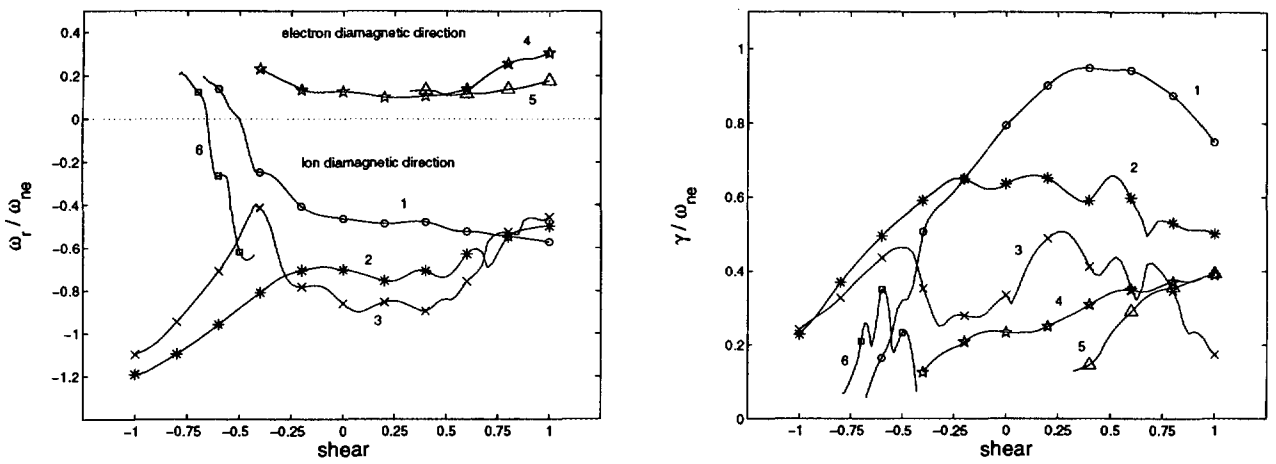

Figure 3: Real frequencies ω_r and growth rates γ as a function of shear $\hat{s}$ for a sampling of unstable eigenmodes, non-adiabatic trapped electron dynamics being taken into account. For $\hat{s}= +1.0$ the unstable spectrum contains simultaneously positive and negative frequencies. At $\hat{s}= -1.0$ only the ITG-type modes remain destabilized, however with a significantly reduced growth rate compared with the highest one around $\hat{s}= +0.5$.

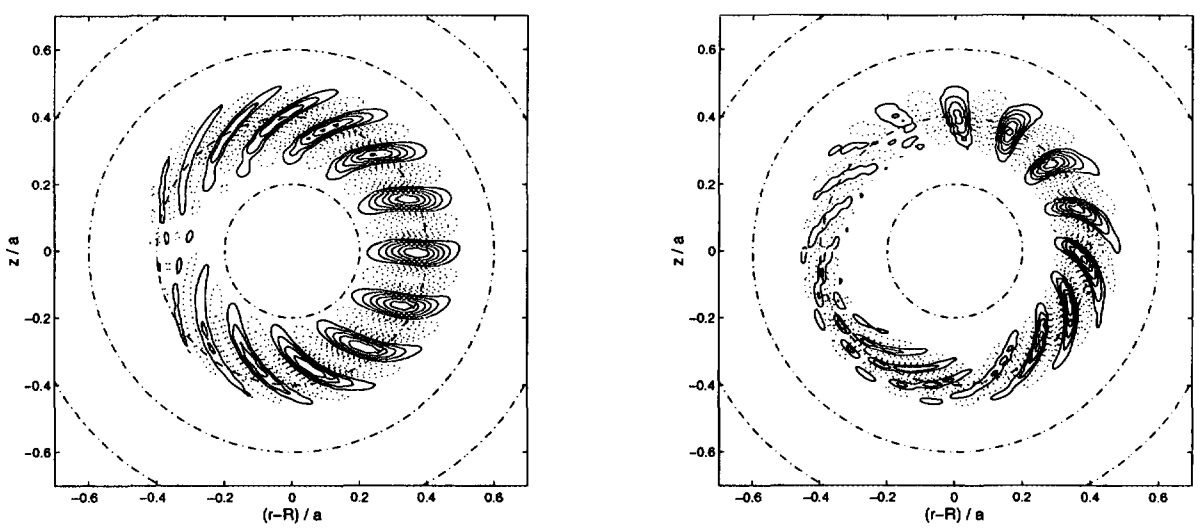

a.) $\hat{s}= +1.$ e.) $\hat{s}= -1.$

Figure 4: Mode structures of most unstable toroidal-ITG-type eigenmodes along shear scan $\hat{s}= +1. \ldots . - 1.$

to $\hat{s}$= 0.5. Negative shear stabilizes the toroidal-ITG by twisting the convective cells more rapidly into a vertical position where they are less effectively driven[18]. This appears clearly in the poloidal mode structures of Fig.4 (axis of symmetry on the left). The TEM's are stabilized by reversal of the average toroidal precessional drift of the trapped particles. Thus realistic negative magnetic shear alone does not seem to be sufficient to explain the dramatic improvement of confinement in negative central shear discharges. Experimental results[16] point towards the $\vec{E} \times \vec{B}$ flow shear for being responsible for the full stabilization of microinstabilities[19].

References

[1] J.W.Connor, R.J.Hastie, and J.B.Taylor, Physical Review Letters **40**, 396 (1978).

[2] R.Marchand, W.M.Tang, and G.Rewoldt, Physics of Fluids **23**, 1164 (1980).

[3] W.M.Tang and G.Rewoldt, Physics of Fluids B **5**, 2451 (1993).

[4] S.E.Parker, W.W.Lee, and R.A.Santoro, Physical Review Letters **71**, 2042 (1993).

[5] M.Kotschenreuther, W.Dorland, M.A.Beer, and G.W.Hammett, Physics of Plasmas **2**, 2381 (1995).

[6] S.Brunner, Ph.D. thesis, Ecole Polytechnique Fédérale de Lausanne, 1997.

[7] P.J.Catto, Plasma Physics **20**, 719 (1978).

[8] M.Rosenbluth and M.L.Sloan, Physics of Fluids **14**, 1725 (1971).

[9] B.Davies, Journal of Computational Physics **66**, 36 (1986).

[10] M.Fivaz *et al.*, Physical Review Letters **78**, 3471 (1997).

[11] M.Fivaz, Ph.D. thesis, Ecole Polytechnique Fédérale de Lausanne, 1997.

[12] S.Brunner *et al.*, in *Theory of Fusion Plasmas, Int. Workshop, Varenna, August 1996* (Editrice Compositori, Societa Italiana di Fisica, Bologna, 1997), p. 101.

[13] J.Q.Dong, W.Horton, and J.Y.Kim, Physics of Fluids B **4**, 1867 (1992).

[14] F.Romanelli and S.Briguglio, Physics of Fluids B **2**, 754 (1990).

[15] F.M.Levinton *et al.*, Physical Review Letters **75**, 4417 (1995).

[16] L.L.Lao *et al.*, Physics of Plasmas **3**, 1951 (1996).

[17] Y.Neyatani and the JT-60 Team, Plasma Physics and Controlled Fusion **38**, A181 (1996).

[18] T.M.Antonsen Jr. *et al.*, Physics of Plasmas **3**, 2221 (1996).

[19] T.S.Hahm and K.H.Burrell, Physics of Plasmas **2**, 1648 (1995).